JOURNAL OF VIROLOGY, May 1985, p. 586–597
0022-538X/85/050586-12$02.00/0

Vol. 54, No. 2

Development and Analysis of a Transformation-Defective Mutant of Harvey Murine Sarcoma *tk* Virus and Its Gene Product

MAUREEN O. WEEKS,[1]* GORDON L. HAGER,[2] ROBERT LOWE,[3] AND EDWARD M. SCOLNICK[3]

Laboratory of Tumor Immunology and Biology[1] and Laboratory of Experimental Carcinogenesis,[2] National Cancer Institute, Bethesda, Maryland 20205, and Merck Sharp & Dohme Research Laboratories, West Point, Pennsylvania 19486[3]

Received 19 June 1984/Accepted 1 February 1985

The Harvey murine sarcoma virus has been cloned and induces focus formation on NIH 3T3 cells. Recombinants of this virus have been constructed which include the thymidine kinase gene of herpes simplex virus type 1 in a downstream linkage with the p21 *ras* gene of Harvey murine sarcoma virus. Harvey murine sarcoma *tk* virus rescued from cells transfected with this construct is both thymidine kinase positive and focus inducing in in vitro transmission studies. The hypoxanthine-aminopterin-thymidine selectability of the thymidine kinase gene carried by this virus has been exploited to develop three mutants defective in the p21 *ras* sequence. All three are focus negative and thymidine kinase positive when transmitted to suitable cells. Of these, only one encodes a p22 that is immunologically related to p21. This mutant has been used to explore the relationship between the known characteristics of p21 and cellular transformation. Data presented herein indicate that the p21 of Harvey murine sarcoma virus consists of at least two domains, one which specifies the guanine nucleotide-binding activity of p21 and the other which is involved in p21-membrane association in transformed cells.

That the 21,000-molecular-weight (M.W.) p21 protein of Harvey murine sarcoma virus (HaMSV) is associated with cellular transformation has been known for some time (7, 19, 42); together with other *ras*-encoded proteins it has been implicated in the ontogeny of bladder, lung, and colon cancer as well as in neuroblastoma (11, 26, 29, 44, 45). Furthermore, activation of the normal cellular *ras* homolog by bringing it under the control of the HaMSV viral promotor results in cellular transformation in transfection studies (5, 10). It has been suggested that the transformation phenomenon is a result either of increased expression of *ras* gene products (5, 6, 10, 14, 35, 46) or of conformational changes induced by the alteration of a single amino acid in the transforming gene product due to a point mutation within the encoding DNA sequence (12, 27, 48, 49, 51, 53).

Attempts at developing HaMSV mutants with which to explore the transformation of cells as mediated by the expression of the 21,000-dalton viral protein (p21) have been limited. The difficulty encountered in looking for this type of mutant has been that there was no easy way to monitor for the presence of inactive HaMSV genes or genes exhibiting low levels of expression in this system; as HaMSV possesses no characteristic features other than the expression of p21, loss or alteration of p21 expression has therefore meant loss of viral identity in infected cells.

Wei et al. (52) reported the construction of a derivative of HaMSV which incorporates a functional thymidine kinase gene from herpes simplex virus type 1 in a downstream linkage with the transforming or p21-encoding region of HaMSV; this derivative is HaMSVtk5. In this paper we report both the use of the HaMSVtk virus to develop transformation-defective mutants in the *ras* gene with 5-bromodeoxyuridine and the nature of the resultant mutations.

* Corresponding author.

MATERIALS AND METHODS

Cells and viruses. Fibroblasts were grown in Dulbecco-Vogt modified Eagle minimal essential medium containing 10 U of penicillin per ml and 100 μg of streptomycin per ml (DMEM) and 10% fetal calf serum. Transformed cells were grown initially in DMEM–Ham F12 (1:1)–7.5% horse serum. All cells were grown in incubators maintained at 37°C and 10% CO_2. Cells containing the viral thymidine kinase gene were grown in hypoxanthine-aminopterin-thymidine (HAT) medium (DMEM–10% fetal calf serum supplemented with 10^{-5} M hypoxanthine, 4×10^{-7} M aminopterin, and 1.6×10^{-5} M thymidine [47]).

The following cells were used in this study: NIH 3T3, a highly contact-inhibited fibroblast line derived from NIH Swiss mouse embryo cultures (22); NIH 3T3 (TK^-), a thymidine kinase-deficient clonal NIH 3T3 cell line obtained from Robert Goldberg, Merck Sharp & Dohme Research Laboratories, West Point, Pa.; B21, a second contact-inhibited thymidine kinase-deficient cell line derived from BALB/c embryo cultures (20); and 543 C19, a subclone of the original NIH 3T3 cell line nonproductively transformed by HaMSVtk (52).

Viruses used were 21-1S, an ecotropic Moloney murine leukemia virus provided by Char-mer Wei, formerly of the National Cancer Institute, Bethesda, Md.; 543 C19 21-1S, a subclone of the original HaMSVtk virus derived by superinfection of 543 C19 cells and rescue of HaMSVtk from these cells with 21-1S; FMuLV 543 C19, HaMSVtk rescued by the Friend strain of murine leukemia virus (50); and FMuLV Ha821, HaMSV rescued by the Friend strain of murine leukemia virus (40). Titers of transforming virus were determined by the focus formation assay on freshly infected NIH 3T3 cells as described by Jainchill et al. (22). Leukemia virus titers were determined by the XC plaque test reported by Rowe et al. (28).

Viral mutagenesis. NIH 3T3 cells seeded in DMEM–10% fetal calf serum plus 5 μg of polybrene were infected with the

543 C19 21-1S virus at a multiplicity of 0.1. Included in the medium for viral infection were various concentrations of 5-bromodeoxyuridine (0, 10, 20, 50, 100, and 200 μg/ml). After 72 h, all plates were exposed to white light for 1 h before the medium was replaced with fresh DMEM–10% fetal calf serum. Viral harvests were made at 24 and 48 h and stored at −70°C until they were used (37).

Selection for viral mutants. NIH 3T3 (TK−) cells were infected with potentially mutagenized 543 C19 21-1S viral stocks at log-scale dilutions (10^{-1} through 10^{-4}). After 24 h, infected cells were fed with HAT selective medium (47). Conditions were chosen that would give rise to 10 thymidine kinase CFU/60-mm plate. Mutagenized viral clones were isolated by using the following conditions: (i) adsorption of potentially mutagenized virus onto B21 cells was allowed for 1 h at 37°C; (ii) cultures were fed with DMEM–10% fetal calf serum; (iii) 24 h later, infected cells were treated with 0.1% trypsin–1 mM EDTA for 10 min at 37°C and plated in 96-well microtiter plates; (iv) single cells were grown up in DMEM–10% fetal calf serum; and (v) clonal selection was then based on flat morphology and continued growth when transferred into HAT medium.

Cell labeling and lysate immunoprecipitation. Cell lines for labeling were grown to approximately 80% confluency in either HAT medium or DMEM–10% fetal calf serum. Labeling conditions with L-[^{35}S]methionine or $^{32}P_i$ have been described elsewhere (43). The labeling medium was removed, and the cells were washed twice with cold phosphate-buffered saline. Lysis was carried out in situ with 1 ml of BW buffer without sodium dodecyl sulfate (SDS) (1% Triton X-100, 0.5% deoxycholate, 0.01 M sodium phosphate [pH 8.0], 0.1 M NaCl, 1 mM EDTA). Lysates were centrifuged at 4°C for 30 min at 100,000 × *g*. The supernatant was recovered and incubated with 250 μl of coated Staph A (16)–15 μl of normal rat serum at 4°C. After 2 to 4 h, the mixture was centrifuged at 10,000 × *g* for 10 min at 4°C. Trichloroacetic acid-precipitable counts were determined on a sample of the supernatant, and the remainder was stored at −20°C. This procedure has been described with minor modifications by Shih et al. (42). Radiolabeling with [9,10-^{3}H(N)]palmitic acid was performed for a minimum of 15 h in accordance with Sefton et al. (38).

The immunoprecipitation protocol was modified from that of Furth et al. (16). Monoclonal antibody (10 μl) made to HaMSV p21 (YA6-238 or Y13-172) was mixed with 5×10^6 to 20×10^6 trichloroacetic acid-precipitable cpm of labeled cell lysate in a 1.5-ml Eppendorf microfuge tube and adjusted to 300 μl with BW buffer without SDS. The reaction mixture was incubated for 2 h at 4°C. The addition of 50 μl of coated Staph A was followed by an additional 1 h of incubation at 4°C. The reaction mixture was centrifuged at 10,000 rpm for 1 min in an Eppendorf 5413 microfuge to collect the immune complex. The resultant Staph A pellet was suspended, washed five times with 1.0 ml of cold BW buffer, and centrifuged. After the final wash, pellets were suspended in 25 μl of SDS sample buffer (100 mM Tris-hydrochloride [pH 6.8], 2% SDS, 2% 2-mercaptoethanol, 40% glycerol, 0.004% bromphenol blue), boiled for 3 min, and centrifuged for 5 min to remove dissociated Staph A. Discontinuous slab gel electrophoresis of proteins was carried out by the method of Laemmli (23) with 12% SDS–polyacrylamide separating gels. Gels were fixed in 10% acetic acid–25% 2-propanol overnight at room temperature. Gels containing proteins labeled with L-[^{35}S]methionine were soaked twice in dimethyl sulfoxide for 30 min each. Gels then were impregnated with 2,5-diphenyloxazole by soaking in a solution of 22% 2,5-diphenyloxazole in dimethyl sulfoxide for 2 h at 37°C. Finally the gels were washed in cold water for 1 h and dried. Gels containing ^{32}P-labeled protein were simply fixed and dried. Dried gels then were autoradiographed (1).

Protein size designations were made in reference to the mobilities of ^{14}C-labeled protein standards (Bethesda Research Laboratories, Rockville, Md.).

Subcellular localization of viral gene products. Subcellular fractionation of infected and uninfected cells was performed essentially by the method of Courtneidge et al. (9). Labeled and unlabeled cell extracts were treated identically. Cells were scraped into phosphate-buffered saline and washed. Packed cells were suspended in 10 volumes of 0.01 M Tris-hydrochloride (pH 8.0)–0.1 mM dithiothreitol. They were disrupted with 20 strokes with a Wheaton overhead stirrer to propel a Dounce homogenizer. The nuclear fraction was removed by centrifugation at 600 × *g* for 15 min at 4°C, and the supernatant was centrifuged at 100,000 × *g* for 30 min at 4°C. Recovered supernatant or S100 was adjusted to 1.0% Triton X-100. The pellet or P100 fraction was suspended in 0.01 M Tris-hydrochloride (pH 8.0)–0.1 mM dithiothreitol–1% Triton X-100 and disrupted by passage three times through a 22.5-gauge needle. Particulate matter was removed by centrifugation for 10 min at 10,000 × *g*. Extracts then were concentrated and purified by precipitation with an equal volume of saturated ammonium sulfate at 4°C. The precipitate was centrifuged at 100,000 × *g* for 30 min at 4°C. The precipitate (found on the walls of the centrifugation tubes) was suspended in 0.01 M Tris-hydrochloride (pH 7.5)–0.1% Triton X-100 and dialyzed extensively against 0.01 M Tris-hydrochloride (pH 7.5).

Enzymatic analysis of protein products. The tryptic peptide mapping procedure described by Shih et al. was followed precisely (40). Samples for *Staphylococcus aureus* V8 cleavage were excised from gels and digested with 1 or 5 μg of *S. aureus* V8 protease (Miles Laboratories, Inc., Elkhart, Ind.) at 25°C for 90 min. Products of enzymatic cleavage were analyzed on 15% SDS-polyacrylamide gels and autoradiographed (8, 40).

Phosphoamino acid analysis. Phosphate-labeled protein electrophoresed on SDS-polyacrylamide gels was eluted from unfixed gels as described previously (40). Eluted protein was hydrolyzed at 110°C for 3 h in 6 N HCl. Samples were lyophilized twice and suspended for the first dimension in 5 μl of the electrophoresis buffer (glacial acetic acid:formic acid:water, 78:25:897). Unlabeled internal markers included in this mixture (phosphothreonine, phosphoserine, and phosphotyrosine) were supplied by Thomas Shih, National Cancer Institute. Samples were spotted on Schleicher & Schuell G 1440 thin-layer chromatography plates and electrophoresed at 950 V for 90 min. Ascending chromatography, the second dimension, was carried out in 0.5 M ammonium hydroxide–isobutyric acid (3:5, vol/vol). The ^{32}P-phosphoamino acids were visualized by autoradiography, and the internal markers were visualized by ninhydrin staining (13).

Guanine nucleotide-binding assay for protein activity. Samples of p21 and related proteins were purified by subcellular fractionation as described above. The protein concentrations were determined by the method of Lowry et al. (24). Up to 1,600 μg of protein was mixed with 5×10^{-6} M [8-^{3}H]GDP in 0.6 ml of GDP binding buffer (1% Triton X-100, 0.1 M NaCl, 0.005 M $MgCl_2$, 0.05 M Tris-hydrochloride [pH 7.6]) with 7 μl of HaMSV-specific monoclonal antibody (YA6-238)–65 μl of protein A-Sepharose coated

with rabbit antibody to rat immunoglobulin G. The last reagent, protein A-Sepharose C1-4B, had been reconstituted in 14 volumes of GDP binding buffer and coated in the manner described for Staph A. Incubation was carried out at 4°C with a Tektator V shaker for agitation. After incubation, the immune complexes were collected by centrifugation and washed three times with GDP- and $MgCl_2$-free binding buffer. The complexes were collected on 0.45-μm filters (Millipore Corp., Bedford, Mass.) and washed an additional three times with the same buffer at 4°C, and the filters were dissolved in 15 ml of Filtron-X (National Diagnostics, Somerville, N.J.). The amount of [8-^{3}H]GDP retained was determined by liquid scintillation counting. In these experiments 13,100 cpm was equivalent to 1 pmol of [8-^{3}H]GDP (16, 36).

In vitro ^{32}P-labeling of proteins by autophosphorylation. Protein from the S100 or P100 fractions was labeled with ^{32}P donated by [γ-^{32}P]GTP in the following reaction. Samples were immunoprecipitated as described above. The Staph A bound immune complex was washed in GDP binding buffer and incubated for 30 min at 37°C in 25 μl of 0.1 M NaCl–0.005 M $MgCl_2$–0.05 M Tris-hydrochloride (pH 8.0). Included in the mixture was 1 mM [γ-^{32}P]GTP. At the conclusion of the incubation, an equal volume of SDS-polyacrylamide gel sample buffer was added, and the samples were boiled for 3 min and electrophoresed on 12% SDS-polyacrylamide gels. Phosphate-labeled proteins were visualized by autoradiography (40).

RESULTS

As described above, 24-h viral harvests from NIH 3T3 cells infected with 543 C19 21-1S were used to infect fresh NIH 3T3 cells in the presence of various levels of 5-bromodeoxyuridine. Cells were exposed to white light and then refed, and 24- and 48-h viral harvests were made. After preliminary characterization of potentially mutagenized virus on NIH 3T3 (TK$^-$) cells, the 48-h viral stock made from plates subjected to 20 μg of 5-bromodeoxyuridine was judged to result in sufficient infected cell mortality in HAT medium to make further studies practical. A sufficient mortality rate represented a 2-log reduction in virally induced thymidine kinase colony-forming and focus-forming activities in the appropriate cells.

Selection and characterization of viral mutants. As indicated above, B21 cells were infected with potentially mutagenized 543 C19 21-1S virus at a 1:100 dilution, that condition established in preliminary studies known to give rise to 10 thymidine kinase CFU/ml of virus applied to a 60-mm plate. Infected cells were plated in 96-well microtiter plates, and clones were selected by virtue of their growth in HAT medium. A total of 400 clones infected with potentially mutagenized HaMSVtk virus were isolated in this manner. Of these, three independently derived clones were recovered which had survived in HAT medium and were not morphologically transformed. These viral clones, designated 729 C19, 729 C120, and 729 C145, were picked and propagated in HAT medium.

Viral supernatants from 729 C19, 729 C120, and 729 C145 were used to infect fresh NIH 3T3 cells and NIH 3T3 (TK$^-$) cells. This was done both to ensure that transmissible retrovirus had been recovered and to determine viral titers in focus formation and thymidine kinase colony formation. The titer of the Moloney murine leukemia virus helper virus present in infected cells also was determined by XC plaque assay of Rowe et al. (28).

The parental or wild-type Moloney murine leukemia virus-HaMSVtk (543 C19 21-1S) virus expresses approximately equal levels of thymidine kinase CFU and focus-forming units per milliliter (Table 1). Clones 729 C19, 729 C120, and 729 C145 have no demonstrable focus-forming activity but do express similar levels of thymidine kinase colony formation. All four lines are active in the XC plaque-forming assay, although disparity is clearly visible between the numbers of CFU and PFU in some cases. The Moloney murine leukemia virus control (21-1S) is active only in the plaque-forming assay as would be expected. Uninfected cells used as an absolute control for these studies have no observable activity in any of the assays.

TABLE 1. Titers of viral activity of transformation-defective viruses related to HaMSVtk

Virus	FFU per ml on NIH 3T3 cells	tk$^+$ colonies per ml on NIH 3T3 (TK$^-$) cells	PFU[b]/ml
543 C19 21-1S	1.0×10^6 to 5.0×10^6	4.5×10^6	4×10^7
729 C19	0.0	4.0×10^6 to 10.0×10^6	1.4×10^7
729 C120	0.0	1.5×10^6	5.6×10^6
729 C145	0.0	4.5×10^5	5.0×10^5
21-1S	0.0	0.0	1.0×10^7
Control	0.0	0.0	0.0

[a] FFU, Focus-forming units.
[b] Determined by the XC plaque assay of Rowe et al. (28).

Characterization of recovered viral mutants. Uninfected B21 cells and cells infected with viral mutants 729 C19, 729 C120, or 729 C145 were pulse-labeled with L-[^{35}S]methionine to determine whether p21-related proteins were being synthesized in these cells. Also, to ascertain whether the parental HaMSVtk cells did indeed produce a transforming protein identical to that found in HaMSV-infected cells, pulse-labeling was performed in cells infected with FMuLV Ha821 as well. Labeling was carried out for 15 h at 37°C. Lysates were prepared as described above, immunoprecipitated with monoclonal antibody specific for p21 (YA6-238), and electrophoresed on 12% SDS-polyacrylamide gels for 6 h at 120 V.

Immunoprecipitates of FMuLV Ha821-infected cells produce the characteristic p21 and pp21 doublet (Fig. 1A, lane 2). A doublet of the same mobility is also seen in cells infected with 543 C19 21-1S (Fig. 1B). In cells infected with clone 729 C19, however, a doublet of slower mobility is seen (Fig. 1C). This doublet consists of a 22,000-M.W. protein, p22, and a slower migrating species with a M.W. of 23,000. No p21-related protein is seen in immunoprecipitates from cells infected with clone 729 C120 or 729 C145 or in uninfected B21 cells (Fig. 1D, E, and F).

In concert with the pulse-labeling of infected cells with [^{35}S]methionine, a separate but identical study was performed with $^{32}P_i$ (Fig. 2). FMuLV Ha821-infected cells produce a phosphoprotein pp21 with a mobility equal to that of the upper band in the [^{35}S]methionine-labeled doublet (Fig. 2A). The same is true for cells infected with 543 C19 21-1S (Fig. 2B). 729 C19-infected cells have a phosphoprotein of 23,000 M_r. The mobility pattern seen here is like that of the upper band of the characteristic p21 doublet, and this phosphoprotein will be called pp22.

Examination of protein synthesis and processing. The p22 encoded by the 729 C19 virus demonstrates a mobility intermediate to that of the bands representing the characteristic [^{35}S]methionine p21 doublet of HaMSV. However, it is

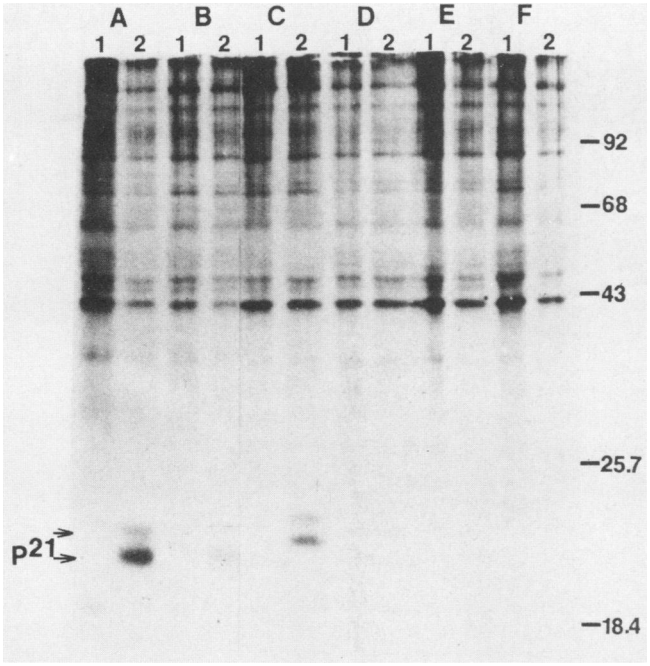

FIG. 1. Immunoprecipitates from [^{35}S]methionine-labeled cells infected by transformation-defective viruses. Lysates from cells labeled with [^{35}S]methionine for 15 h were prepared and analyzed by electrophoresis on 12% SDS-polyacrylamide gels, followed by autoradiography. Lysates (10^6 cpm) were immunoprecipitated in the absence (lane 1) and presence (lane 2) of monoclonal antibody specific for HaMSV p21. Lysates from cells infected with the following viruses are shown: A, FMuLV Ha821; B, 543 C19 21-1S; C, 729 C19; D, 729 C120; E, 729 C145. Section F shows immunoprecipitates prepared from lysates of uninfected B21 cells. The p21 doublet is indicated. Size markers are indicated in kDa.

known that p21 pulse-labeled with [^{35}S]methionine for very short periods of time is detected in a precursor form (pro-p21) with a M.W. of 22,000. As the duration of labeling increases, pro-p21 is cleaved to give the mature p21, and at 24 h, phosphorylated pp21 has appeared (41). To determine whether this is also true of p22 in 729 C19-infected cells, labeling with [^{35}S]methionine was carried out for 15 min, for 1, 2, 4, and 24 h. Lysis and immunoprecipitation were performed as described above, and immunoprecipitates were analyzed on 12% SDS-polyacrylamide gels. Immunoprecipitates from FMuLV Ha821, 543 C19 21-1S, 729 C19, and 729 C145 were prepared in parallel (Fig. 3). Panels I and II represent material immunoprecipitated in the presence and absence, respectively, of monoclonal antibody YA6-238. Immunoprecipitates from FMuLV Ha821-infected cells demonstrate typical processing of p21 (Fig. 3I, section A). Pro-p21 is the principal species present in cells labeled for 15 min. At 1 h pro-p21 is still present and p21 has begun to appear. The proportion of mature p21 increases up to 4 h as the relative amount of pro-p21 decreases. At 24 h, phosphorylated p21 has appeared. Immunoprecipitates from cells infected with 543 C19 21-1S exhibit the same pattern (Fig. 3I, lane B).

Lysate from 729 C19-infected cells expresses a p22 that is synthesized as a 22,000-M.W. protein and does not undergo any detectable change until the phosphorylated form, pp22, appears within 24 h (Fig. 3I, section C). It can be seen that p22 exhibits the same mobility shown by pro-p21 in adjacent sections of panel I (Fig. 3). As expected, immunoprecipitates of 729 C145 (Fig. 3I, section D) exhibit no p21-related species at any time.

Subcellular localization. 543 C19 21-1S-, 729 C19-, and 729 C145-infected cells pulse-labeled with L-[^{35}S]methionine were homogenized and partitioned into a cytosol fraction (S100) and a particulate or membrane fraction (P100). Immunoprecipitation was carried out on each fraction together with total cell extracts by using monoclonal YA6-238. Analysis was performed with 12% SDS-polyacrylamide gels (Fig. 4). Panel A shows the p21 fractionation pattern of cells infected with 543 C19 21-1S. It is clearly visible that the p21-pp21 doublet can be detected in total cell lysate and in the membrane or P100 fraction. Panel B indicates that p22-pp22 from 729 C19-infected cells is present in total cell extract and in the S100 or cytosol fraction. It does not appear in the membrane fraction. When these results are compared with those of Shih et al. (41), mutant p22 is seen to demonstrate the cellular fractionation pattern shown by pro-p21. Panel C represents the 729 C145 cell extracts used as a negative control.

Analysis of protein cleavage products. Tryptic digestion of [^{35}S]methionine-labeled p21 from HaMSVtk-infected cells yields more than the expected number of peptides. This conclusion is based on the number of methionine-containing tryptic peptides predicted from the DNA sequence of v-Ha-*ras* (12). Incomplete digestion by trypsin or cleavages at residues other than arginine and lysine may account for this. Alterations in the length of incubation or amount of trypsin used for digestion have been explored as a means to remedy this effect (40). However, the purpose of this experiment was to determine that the tryptic peptides generated from

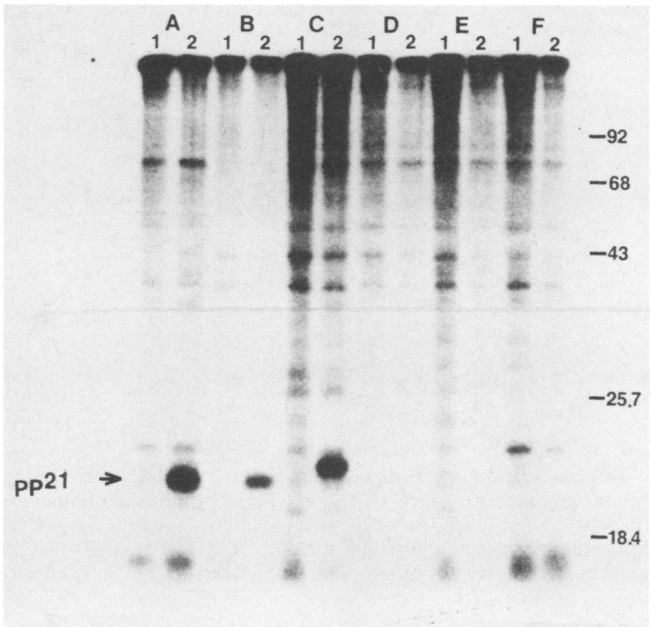

FIG. 2. Immunoprecipitates from $^{32}P_i$-labeled cells infected by transformation-defective viruses. Lysates from cells labeled with $^{32}P_i$ for 15 h were prepared and analyzed by electrophoresis on 12% SDS-polyacrylamide gels, followed by autoradiography. Lysates (0.2% of the total lysate volume) were immunoprecipitated in the absence (lane 1) and presence (lane 2) of monoclonal antibody specific for HaMSV p21. Lysates from cells infected with the following viruses are shown: A, FMuLV Ha821; B, 543 C19 21-1S; C, 729 C19; D, 729 C120; E, 729 C145. Section F shows immunoprecipitates prepared from lysates of uninfected B21 cells. Phosphorylated p21 is indicated. Size markers are indicated in kDa.

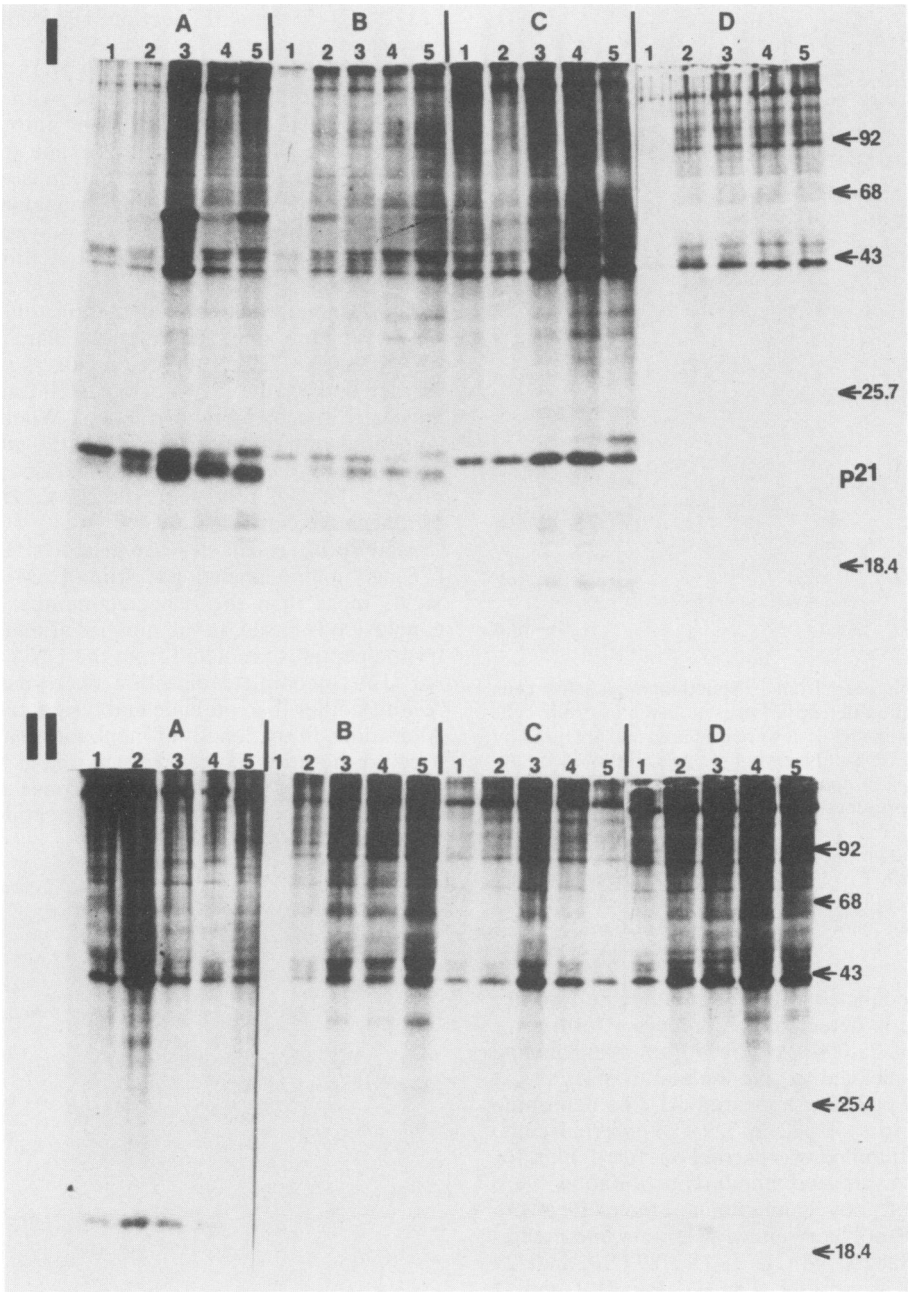

FIG. 3. Protein processing in cells infected with wild-type and transformation-defective viruses. Immunoprecipitation was performed on lysates prepared from cells that were labeled with [^{35}S]methionine for 15 min and 1, 2, 4, and 24 h (lanes 1 to 5, respectively) in the presence (panel I) and absence (panel II) of monoclonal antibody specific for HaMSV p21. Lysates were prepared from B21 cells infected with the following viruses: A, FMuLV Ha821; B, 543 C19 21-1S; C, 729 C19; D, 729 C145. Analysis was by electrophoresis on 12% SDS-polyacrylamide gels, followed by autoradiography. Size markers, in kDa, used in the determination of mobility are indicated, as is the location of p21.

HaMSVtk p21 and those generated by cleavage of 729 C19 p22 under the same conditions were not widely variant. For this reason, HaMSVtk p21 or mutant p22 partially purified by SDS-polyacrylamide gel electrophoresis was digested exactly as described previously (40). This was performed separately on each protein and on a one-to-one mixture of both.

Examination of the peptide map produced from 543 C19 p21 or from 729 C19 p22 reveals that there are two major peptides and a variety of minor peptides whose patterns are very similar but may not be identical (Fig. 5A and C). Digestion of a mixture of the two proteins, however, reveals that the peptides generated by each protein do indeed have the same mobilities in this system (Fig. 5B). This would indicate that the sequences of these proteins are very similar, although there may be differences in regions that do not contain methionine.

A similar study was performed with $^{32}P_i$-labeled p21 and p22. In this case there seem to be three principal phosphopeptides that have a similar distribution pattern (Fig. 6). Three

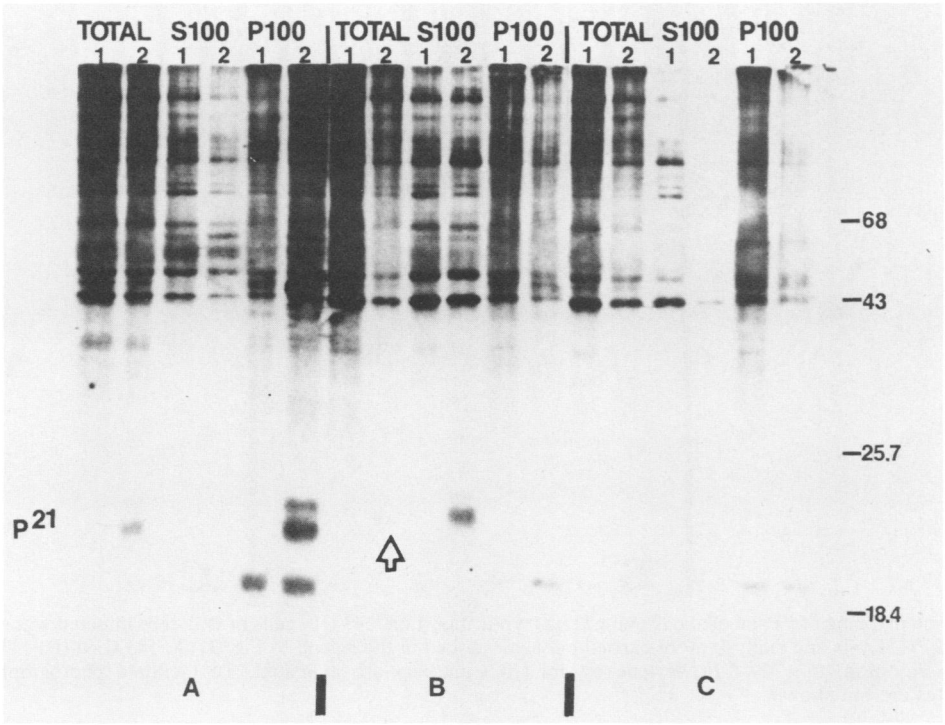

FIG. 4. Localization of p22 by subcellular fractionation. Cells labeled with [^{35}S]methionine were fractionated into an S100 (cytosol) or P100 (membrane) and immunoprecipitated (5×10^6 cpm) in the absence (lane 1) or presence (lane 2) of HaMSV p21-specific monoclonal antibody together with total lysate prepared at the same time. Lysates were prepared from B21 cells infected with the following viruses: A, 543 C19 21-1S; B, 729 C19; C, 729 C145. Analysis was by electrophoresis on 12% SDS-polyacrylamide gels, followed by autoradiography. Size markers, in kDa, used in the determination of mobility are indicated, as is the location of p21. The location of p22 in total extract is shown by an arrow.

minor species are also visible. All six phosphopeptides coincide in tryptic digestions of mixtures of pp21 and pp22.

It is known that the carboxy-terminal difference between p21 and pro-p21 can be demonstrated by differences in the *S. aureus* V8 cleavage of these proteins (41). The difference resides in a 13-kilodalton (kDa) peptide which has been localized by amino acid sequencing to the carboxy-terminal half of the p21 molecule. Comparison of such digests of [^{35}S]methionine-labeled p21 and p22 with either 1 g or 5 μg of *S. aureus* V8 for 90 min at 25°C is shown (Fig. 7). Analysis with 15% SDS-polyacrylamide gels clearly shows that the peptide resulting from cleavage of p22 is larger than that resulting from cleavage of p21. As it has been shown that there are no extraordinary differences among the tryptic

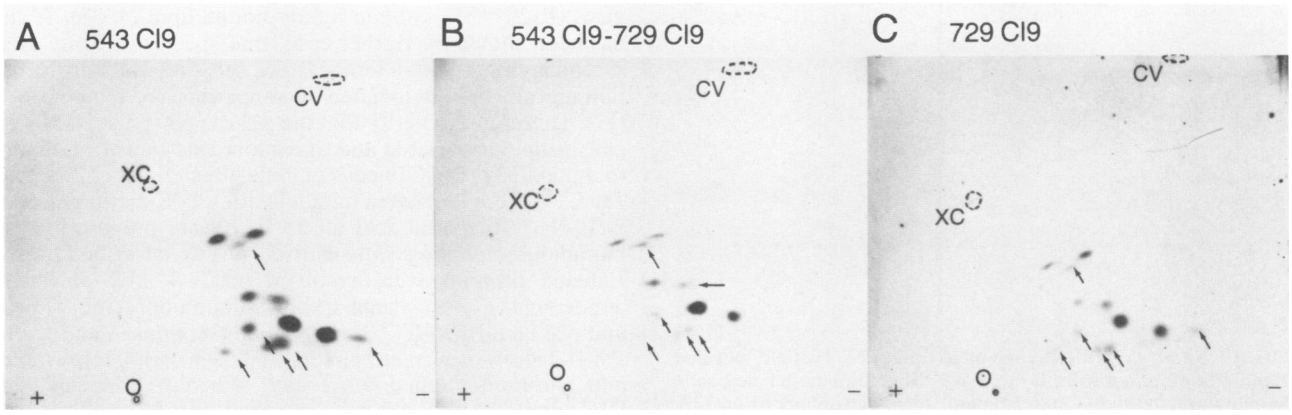

FIG. 5. Comparison mapping of [^{35}S]methionine-labeled p21 and p22 by tryptic digestion. 543 C19 cells or B21 cells infected with 729 C19 were labeled with [^{35}S]methionine for 15 h at 37°C and lysed, and 50×10^6 cpm of labeled protein was immunoprecipitated with HaMSV-specific monoclonal antibody YA6-238. Immunoprecipitates were electrophoresed on 12% SDS-polyacrylamide gels, and p21- or p22-containing bands were excised from gels after autoradiography. The partially purified protein was digested out of the gel slices with three portions of 20 μg of trypsin per ml, lyophilized, and applied to thin-layer chromatography plates at the spots marked with an O. Electrophoresis in the first dimension was from left to right, and chromatography in the second dimension was from bottom to top. (A) 543 C19; (B) 543 C19 mixed with 729 C19 at the time of digestion; (C) 729 C19. Xylene cyanol (XC) and crystal violet (CV) markers are indicated.

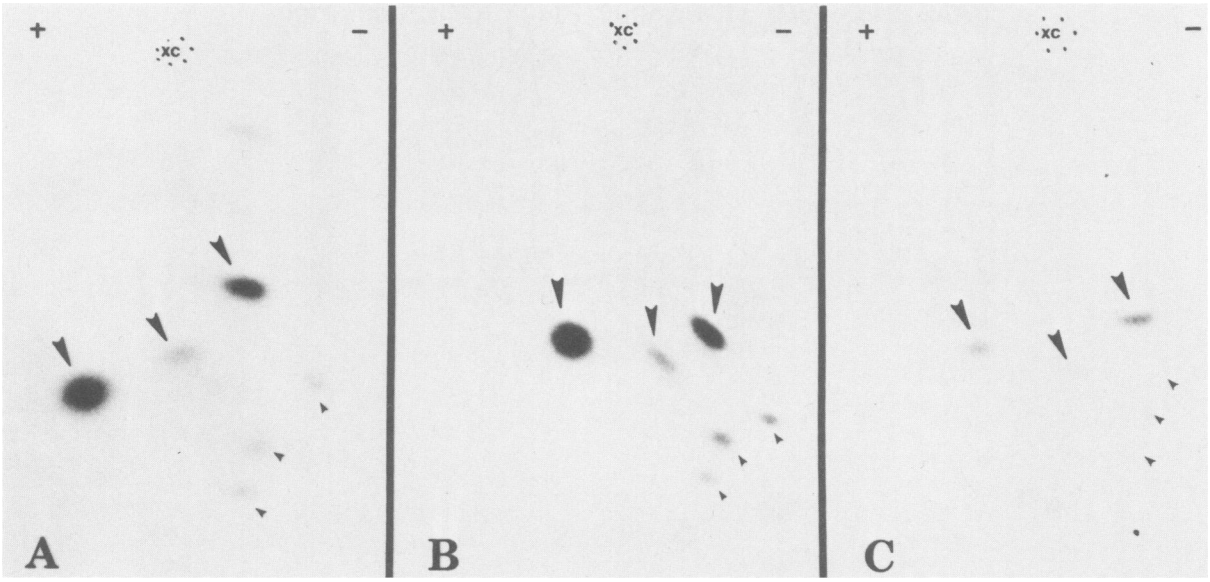

FIG. 6. Comparison mapping of $^{32}P_i$-labeled p21 and p22 by tryptic digestion. 543 C19 cells or B21 cells infected with 729 C19 were labeled with $^{32}P_i$ for 15 h at 37°C. Lysis and analysis were carried out as described in the legend to Fig. 3. (A) 543 C19; (B) 543 C19 mixed with 729 C19 at the time of digestion; (C) 729 C19. Xylene cyanol (XC) markers are indicated. To facilitate photography, whole thin-layer chromatography plates are not shown.

peptides of these two proteins, these results imply that the size difference between p21 and p22 must reside in this carboxy-terminal peptide (41).

Determination of the protein phosphorylation site. The phosphorylation site and surrounding amino acid sequence of HaMSV p21 have been determined by Shih et al. (39, 40). The phosphorylated residue has been found to be threonine residue 59 in the p21 amino acid sequence (12, 39).

Protein samples were prepared by immunoprecipitation of lysate from 543 C19 cells or cells infected with 729 C19 that had been labeled overnight with $^{32}P_i$. Phosphoproteins pp21 and mutant pp22 were eluted from SDS-polyacrylamide gels,

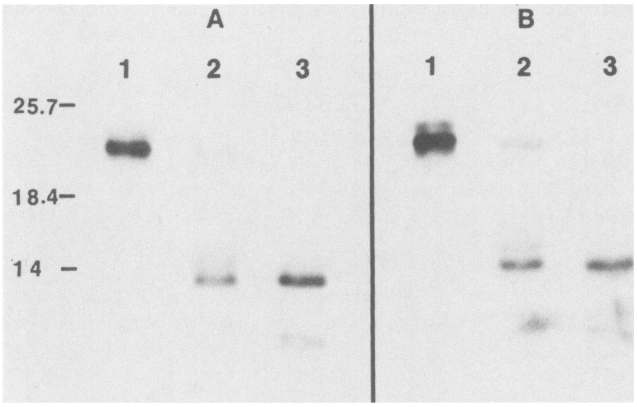

FIG. 7. *S. aureus* V8 cleavage of p21 and p22. Partially purified p21 and p22 prepared from lysates of [^{35}S]methionine-labeled cells by immunoprecipitation (50 × 10^6 cpm) and electrophoresis on 12% SDS-polyacrylamide gels were eluted from wet gels after autoradiography. Samples prepared from 543 C19 cells or cells infected with 729 C19 were digested with 1 or 5 μg of *S. aureus* V8 protease at 25°C for 90 min. Cleavage products were analyzed on 15% SDS-polyacrylamide gels and autoradiographed for 1 week. (A) 543 C19 p21; (B) 729 C19 p22. Lanes: 1, untreated; 2, 1 μg of *S. aureus* V8; 3, 5 μg of *S. aureus* V8. Size markers are expressed in kDa.

lyophilized, and hydrolyzed with 6 N HCl at 110°C for 3 h. By using the two-dimensional analysis system described by Eckhart et al. (13) and comparing the mobility of the isotopically labeled amino acids with that of unlabeled internal phosphoamino acid standards, it can be seen that the residue phosphorylated in 729 C19-infected cells is also threonine (Fig. 8). Traces of phosphoserine can be seen in the mixture of both phosphopeptides (Fig. 8B). This probably represents phosphorylation of cellular p21 (25). What appears to be a large residue to the left of phosphothreonine in Fig. 8 represents incomplete hydrolysis products. The material migrating toward the positive electrode is inorganic phosphate.

Examination of fatty acid association. Buss and Sefton (4) and Sefton et al. (38) have shown that the membrane-associated transforming proteins of Rous avian sarcoma virus ($pp60^{src}$), HaMSV ($p21^{ras}$), and Abelson murine leukemia virus ($P120^{gag\text{-}abl}$) contain tightly bound lipid (4, 38). It also has been shown by Garber et al. that species of Rous avian sarcoma virus that are temperature sensitive for transformation are not lipid associated at nonpermissive temperatures (17). Therefore, to verify that the p21 expressed in HaMSVtk cells is lipid associated and to explore this aspect in relation to mutant p22, 543 C19 cells or cells infected with 729 C19 or 729 C145 were labeled in parallel with L-[^{35}S]methionine and [9,10-^{3}H(N)]palmitic acid for 15 h. Lysate preparation and immunoprecipitation were carried out as described above. Labeled proteins were resolved on 12% SDS-polyacrylamide gels (Fig. 9). Panel 1 shows immunoprecipitated p21 and p22 labeled with [^{35}S]methionine (sections A and B, +). Panel 2 shows the same material labeled with [^{3}H]palmitate and autoradiographed for 1 day. When p21 labeled with [^{3}H]palmitate was autoradiographed for 1 week, it was clearly visible as a doublet (panel 3, + in section A). The p22 does not appear as a palmitate-labeled species at 1 week or in longer exposures (panel 3, + in section B). Cells infected with 729 C145, therefore, do not exhibit any palmitate-labeled p21-related proteins.

Guanine nucleotide binding and autophosphorylation. To

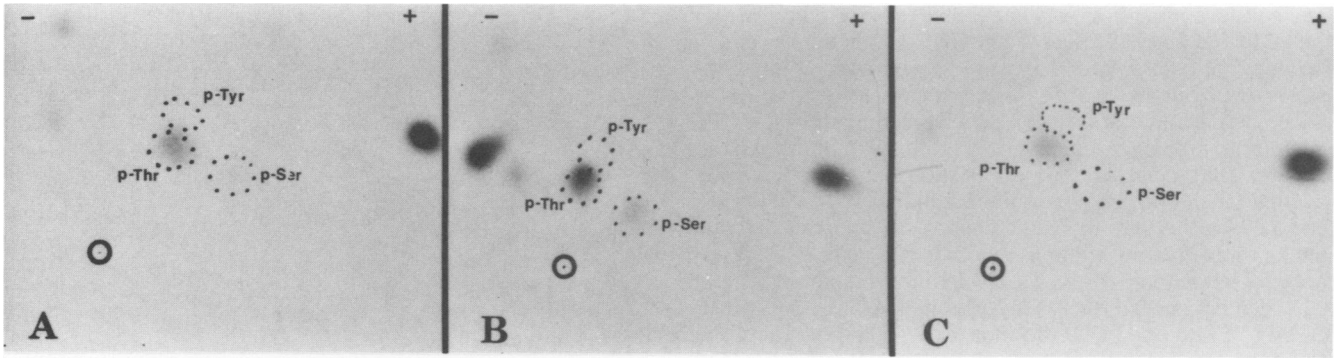

FIG. 8. Phosphoamino acid analysis of p22. Samples of $^{32}P_i$-labeled p21 or p22 were prepared as described in the text (initial lysate, 50 × 10^6 cpm), hydrolyzed in 6 N HCl for 3 h at 110°C, lyophilized, and analyzed in two dimensions, with the internal markers indicated. Electrophoresis in the first dimension is the horizontal direction. Chromatography in the second dimension is from bottom to top. (A) 543 C19 p21; (B) 543 C19 p21 mixed with 729 C19 p22 before hydrolysis; (C) 729 C19 p21. The origin is marked with an O.

ascertain whether the GDP-binding activity associated with $p21^{ras}$ was also associated with the mutant p22 protein, the standard binding assay was performed on extracts of NIH 3T3 cells infected with FMuLV 543 C19, 729 C19, or 729 C145 (16). These lysates represented total extract, S100, and P100 from each cell line. Since preliminary studies showed that nonspecific binding in these extracts was relatively high, extracts were partially purified and concentrated with ammonium sulfate (39). It was assumed that the nucleotide-binding activity would track with the appearance of associated proteins in similar fractionations. The results of binding studies carried out on these preparations are presented (Fig. 10).

It can be seen that extracts of FMuLV 543 C19 do bind GDP in femtomole quantities when prepared under the conditions described. Furthermore, it can be seen that GDP binding by HaMSVtk p21 increases when purified as a P100 cell fraction (Fig. 10). There is no binding activity in an S100 fraction prepared simultaneously.

GDP-binding activity is very low in total extracts of cells infected with 729 C19. As expected, binding activity increases almost sevenfold in an S100 preparation and is almost negative in the corresponding P100 membrane fraction. Binding activity is also lacking in extracts of 729 C145-infected cells at the levels tested.

The published data on total extracts of HaMSV-infected NIH 3T3 cells indicates that 0.9 pmol of [^{3}H]GDP is bound per mg of protein in a total cell extract (39). This translates into 900 fmol/mg or 0.9 fmol/μg. In this assay, the binding activity of HaMSVtk p21 is therefore within the published range. It is also clear that unpurified extracts of cells infected with 729 C19 demonstrate considerably less binding activity.

To verify the specificity of nucleotide binding exhibited by 729 C19 p22, a 20-fold excess (4.1×10^{-5} M) of cold

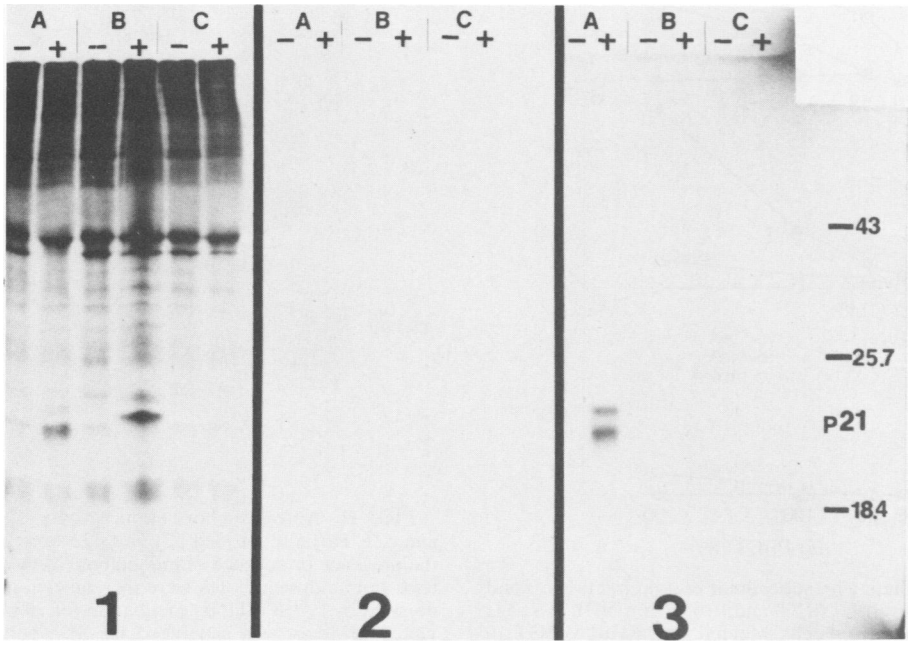

FIG. 9. Labeling of p21 and p22 by [^{3}H]palmitate. Infected B21 cells were labeled with [9,10-^{3}H(N)]palmitic acid for 15 h at 37°C. Lysis and immunoprecipitation of 0.1% of the total lysate was performed in the presence (+) and absence (−) of monoclonal YA6-238 as described in the text. Analysis was by electrophoresis on 12% SDS-polyacrylamide gels, followed by autoradiography for 24 h (panels 1 and 2) or 1 week (panel 3). (A) 543 C19 cell lysate; (B) 729 C19 infected cell lysate; (C) 729 C145 infected cell lysate. Size markers are expressed in kDa.

nucleotide competitor was incubated with either FMuLV 543 C19 P100 or 792 C19 S100 for 30 min before adding labeled [^{3}H]GDP. After the isotope was added, the assay was carried out as usual (Table 2). It can be seen that GDP, GTP, dGDP, and dGTP are effective competitors for the nucleotide-binding site in either p21 or mutant p22. It appears that there are some variations in the effects that adenine nucleotides have on the binding of [^{3}H]GDP by p21 and p22 in this assay, but it cannot be said that adenine nucleotides prevent binding by either p21 or p22. UTP also appears to compete for the GDP-binding site in both p21 and p22. This was also shown by Scolnick et al. (36). GMP, cGMP, TTP, and CTP do not affect binding (data not shown).

The upper band of the p21 doublet has been shown to be phosphate labeled in infected cells and can be labeled in vitro through phosphate donation by [γ-^{32}P]GTP (39, 40). It is also true that HaMSVtk p21 can be autophosphorylated in vitro. Immunoprecipitates of 12 μg (lane 1) or 25 μg (lane 2) of an ammonium sulfate-purified P100 from FMuLV 543 C19-infected cells are shown (Fig. 11A). Samples carried through immunoprecipitation in the absence of monoclonal antibody to p21 are not detected in this assay (lane 3). S100 from 729 C19-infected cells phosphorylates p22 visibly only when immunoprecipitated at the higher concentration (Fig. 11B, lane 2). It is also useful to note that a 30,000-M.W. protein is phosphorylated under these conditions. Such a species has been seen among proteins made from a simian virus 40-HaMSV recombinant that enhances RNA transcription from in-phase initiation sites further upstream in the *ras* gene (18). In the absence of monoclonal antibody no phosphorylation is seen. A P100 prepared from 729 C145-infected cells does not phosphorylate under these conditions.

TABLE 2. Nucleotide competition: [^{3}H]GDP binding

Competitor	[^{3}H]GDP binding (fmol/μg)	
	FMuLV 543 C19 P100	729 C19 S100
GDP	0.038 ± 0.005	0.029 ± 0.029
GTP	0.060 ± 0.014	0.036 ± 0.036
dGDP	0.018 ± 0.011	0.001 ± 0.0005
dGTP	0.037 ± 0.012	0.022 ± 0.017
ATP	0.650 ± 0.090	0.313 ± 0.237
ADP	0.460 ± 0.160	0.212 ± 0.167
dATP	0.560 ± 0.130	0.472 ± 0.377
dADP	0.825 ± 0.175	0.225 ± 0.21
UTP	0.320	0.200 ± 0.070
No competitor	0.825 ± 0.175	0.565 ± 0.395

DISCUSSION

Development of a *ras* gene mutant of HaMSVtk producing p22. It is evident that p22 must possess antigenic determinants intrinsic to p21, as the immunoprecipitability of a p22 doublet when labeled with [^{35}S]methionine has been confirmed. The nonphosphorylated form of this doublet exhibits a mobility intermediate to those of the standard p21 bands and is therefore reminiscent of the pro-p21 precursor protein found in HaMSV-infected cells (41). The possibility that the

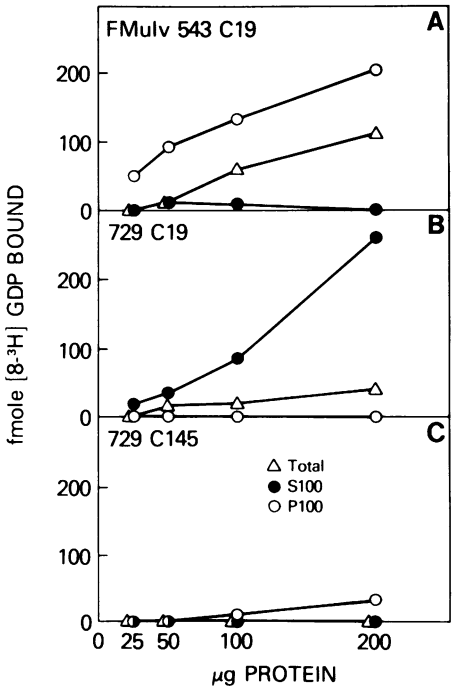

FIG. 10. [^{3}H]GDP binding by subcellular protein fractions. Total lysate and subcellular fractions (S100 and P100) from NIH 3T3 cells infected with 729 C19 and from cells infected with FMuLV 543 C19 were concentrated, partially purified by ammonium sulfate precipitation, dialyzed extensively, and incubated with [^{3}H]GDP. Bound GDP is expressed in femtomoles, where 13,100 cpm = 1 pmol or 1,000 fmol. Protein concentrations are expressed in micrograms.

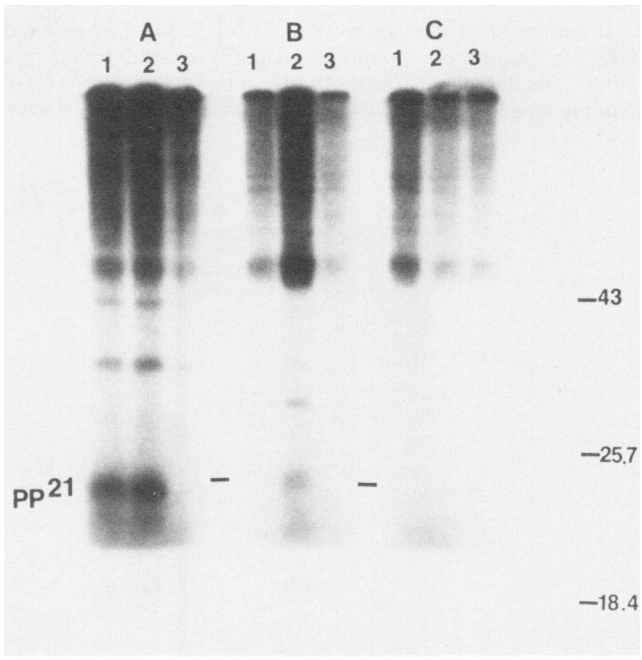

FIG. 11. Autophosphorylation activity of partially purified p21 and p22. Partially purified p21 and p22 were immunoprecipitated in the presence or absence of monoclonal YA6-238 as described in the text. Immunoprecipitates were then labeled in vitro with phosphate donated by [γ-^{32}P]GTP by incubation for 30 min at 37°C. Phosphorylated proteins were analyzed by SDS-polyacrylamide gel electrophoresis, followed by autoradiography. (A) FMuLV 543 C19 P100; (B) 729 C19 S100; (C) P100 from 729 C145. Lanes: 1, 12 μg plus antibody; 2, 25 μg plus antibody; 3, 25 μg without antibody. Size markers are expressed in kDa.

729 C19 virus is a processing-defective mutant of HaMSVtk must therefore be considered. In general, the characterization of p22 should contribute toward an understanding of the relationship between p21 and cellular transformation by helping to identify the cellular target and the transforming functions of p21.

Characterization of a mutant of HaMSVtk producing p22. The development of the p22 mutant of HaMSVtk has several important implications for the study of transforming proteins in relation to cell structure and function. In particular, the characterization of p22 generates certain conclusions about the relationship between p21 and the maintenance of transformation in cells. Therefore, it is necessary to recapitulate the known data on p22 in this context.

It is evident that p22 must possess many of the antigenic determinants intrinsic to p21. Aside from its immunoprecipitability as a doublet when labeled with [^{35}S]methionine, tryptic digestion of p22 produces multiple peptides that appear to be identical to those generated for p21 under the same conditions. Both proteins exist in a phosphorylated form, and threonine is the amino acid phosphorylated in each case (40, 43). Furthermore, the kinetics of phosphorylation in pulse-labeling of cells with $^{32}P_i$ are the same. Tryptic digests of these phosphorylated proteins are highly related as well. This implies that p21 and p22 must also be very similar in amino acid composition. However, it is apparent that p22 demonstrates a reduced mobility with respect to that of p21. Comparison of protein processing, when monitored by labeling with [^{35}S]methionine, indicates that p21 and p22 are both synthesized as "pro-proteins" with an M_r of 22,000. However, although pro-p21 is cleaved to generate the mature p21, the mobility of p22 does not change. Both proteins still give rise to a second protein moiety of decreased mobility within 24 h, and this species comigrates with the band appearing during pulses with $^{32}P_i$ under the same conditions. This could suggest the presence of a mutation within the p22-encoding nucleic acid sequence resulting either in an aberrant cleavage site or in an altered enzyme recognition site preventing enzymatic cleavage from occurring. Furthermore, p22 does not bind palmitate, suggesting a defect at the fatty acid binding site or a processing-membrane association-related failure of p22 to be translocated to the fatty acid binding locus within the cell.

Pro-p21 is synthesized on free ribosomes in cell cytoplasm and can consequently be isolated by crude fractionation of cells into an S100 or cytosol fraction (41). Mature p21 is membrane associated (16, 41, 54). Mature p21 also can be isolated as part of the P100 or membrane fraction of cells. Examination of cells infected with mutant 729 C19 reveals that p22 is found in the S100 from fractionated cells. Comparison of fragments generated from [^{35}S]methionine-labeled p21 and p22 cleavage with *S. aureus* V8 indicates that the size difference between the two proteins is probably at the carboxy terminus of p22 as is true for the size difference between p21 and pro-p21 (41). From this it could be construed that p22 is altered at a membrane binding site or that failure to be cleaved prevents exposure of the necessary binding site. Therefore, these studies imply that p22 is a product of the mutagenized *ras* gene of HaMSV that is defective for protein processing or membrane association. This mutant may be comparable to those developed by Willumsen et al. (55), in which a terminal cysteine residue is altered. However, it is still not clear whether processing or membrane association is the initial event.

It is significant to note that, although cells containing p22 do not undergo transformation, p22 demonstrates GDP-binding activity and is capable of autophosphorylation with [γ-^{32}P]GTP as a phosphate donor. However, p22 appears to differ from p21 in specificity of nucleotide binding. Nucleotide competition studies reveal that p22 has some affinity for adenosine nucleotides that contain multiple phosphate moieties. This could be explained by a gene mutation resulting in amino acid differences in the nucleotide binding site of p22. Alternatively, the failure of p22 to undergo processing may interfere with the folding of the protein. This could result in an altered binding site that possesses the same nucleotide recognition sites but one in which these recognition sites are more flexible with respect to one another. As the presence of trace impurities in the adenine nucleotide stocks used in this assay cannot be excluded entirely, the data presented should be viewed as suggestive rather than conclusive.

The appearance of a transient phosphoprotein pp30 during autophosphorylation of p21 has been noted previously (unpublished data) so its appearance under the same conditions in cell lysates containing p22 is not unusual. As mentioned before, it is known that a p30 can result from the transcription of an open reading frame further upstream in the *ras* gene (12, 18). Phosphorylation of this protein, which may be present at low levels in infected cells, will give rise to the pp30 seen in these studies.

Considerations of p21 and p22 in relation to other *onc* proteins. In these studies we have examined the biochemical properties of a mutant of the *ras* gene that is defective for transformation. This gene is unique in that it produces a protein highly related both structurally and functionally to the transforming protein. The failure of mutant p22 and pp22 to become membrane associated suggests that membrane association is vital to cell transformation.

Several laboratories have demonstrated that a variety of murine retroviral structural (*gag*-gene-encoded) polyproteins undergo posttranslational myristylation (4, 21, 33, 34). The presence of an amino-terminal myristyl-amide linkage enhances the hydrophobicity of these proteins and is thought to facilitate their membrane association (17). Since myristylated amino termini are found in *gag* precursor and cleavage proteins, it is suggested that fatty acid association occurs during protein biosynthesis and must therefore be a prerequisite to membrane association (30–32). A variety of *gag-onc* fusion proteins are also myristylated (33). This suggests that myristylation may play a role (specific membrane attachment) in the transformation process. Palmitate has not been found in association with any of the *gag* polyproteins tested, but palmitate labeling has been used to examine some of the *gag-onc* fusion proteins and with other transforming proteins. Among these are Rous sarcoma virus pp60^{src}, Abelson sarcoma virus P120$^{gag\text{-}abl}$, and HaMSV p21^{ras} (38). Notably, in the case of pp60^{src}, it has been found that labeled palmitate is metabolized to myristate which is found in association with the *onc* gene protein. Therefore, it has been suggested that fatty acid association is necessary for membrane association. This is supported by Garber et al., who found that temperature-sensitive mutants of Rous sarcoma virus fail to be palmitate or membrane associated at nonpermissive temperatures (17).

Fatty acid binding in pp60^{src} and p21^{ras} is posttranslational, occurring in approximately the same time frame as membrane association and cleavage (38). It is not known, however, whether palmitate binding is a prerequisite to or a result of membrane association. The results of Schultz and Oroszlan suggest that lipid binding may be the initial event in the transformation process (33). If so, the principle defect in the p22^{ras} mutant may be failure to bind fatty acid. However,

unpublished data (A. Papageorge, personal communication) suggest that palmitation of p21 occurs in the carboxy-terminal portion of the cleaved molecule. Although the palmitation site has only been localized to the terminal V8 cleavage fragment, one cannot rule out the possibility that an alteration of the p21 cleavage site could also prevent palmitation and interfere with membrane association. That these events are related and associated with transformation by p21 is not contested. It is therefore postulated that p21 contains at least two functional domains, one which is responsible for the nucleotide binding activity and a second which is affected by or results in the cleavage and activation of the mature membrane-bound transforming protein. The mutant protein, p22, has been altered with respect to the second function.

That p21 may consist of more than one domain is not a novel idea. The concept of a transforming protein composed of multiple functional domains (a protein kinase and a second distinct, but necessary, membrane-associated function) is also proposed for the avian *src* protein (2, 3, 15). Whether these domains are *cis* acting in the case of HaMSV p21 is not known for certain at this time (25).

In conclusion, although the time sequence of these events is still unclear, it does appear that transformation in the HaMSV system is correlated with protein processing, membrane association, and lipid binding by the *ras* gene product. Furthermore, the transformation protein of HaMSV consists of at least two domains which must function in tandem for transformation to occur.

ACKNOWLEDGMENT

All work mentioned herein was performed in the Laboratory of Tumor Virus Genetics, National Cancer Institute.

LITERATURE CITED

1. **Bonner, W. M., and R. A. Laskey.** 1974. A film detection method for tritium-labeled proteins and nucleic acids in polyacrylamide gels. Eur. J. Biochem. **46**:83–88.
2. **Bryant, D., and J. T. Parsons.** 1982. Site-directed mutagenesis of the *src* gene of Rous sarcoma virus: construction and characterization of a deletion mutant temperature sensitive for transformation. J. Virol. **44**:683–691.
3. **Bryant, D., and J. T. Parsons.** 1983. Site-directed point mutation in the *src* gene of Rous sarcoma virus results in an inactive *src* gene product. J. Virol. **45**:1211–1216.
4. **Buss, J. E., and B. M. Sefton.** 1985. Myristic acid, a rare fatty acid, is the lipid attached to the transforming protein of Rous sarcoma virus and its cellular homolog. J. Virol. **53**:7–12.
5. **Chang, E. H., R. W. Ellis, E. M. Scolnick, and D. R. Lowy.** 1980. Transformation of cloned Harvey murine sarcoma virus DNA: efficiency increased by long terminal repeat DNA. Science **210**:1249–1251.
6. **Chang, E. H., M. E. Furth, E. M. Scolnick, and D. R. Lowy.** 1982. Tumorigenic transformation of mammalian cells induced by a normal human gene homologous to the oncogene of Harvey murine sarcoma virus. Nature (London) **297**:479–483.
7. **Chang, E. H., J. M. Maryak, C.-M. Wei, T. Y. Shih, R. Shober, H. L. Cheung, R. W. Ellis, G. L. Hager, E. M. Scolnick, and D. R. Lowy.** 1980. Functional organization of the Harvey murine sarcoma virus genome. J. Virol. **35**:76–92.
8. **Cleveland, D. W., S. G. Fisher, M. W. Kirschner, and U. K. Laemmli.** 1977. Peptide mapping by limited proteolysis in sodium dodecyl sulfate and analysis by gel electrophoresis. J. Biol. Chem. **252**:1102–1106.
9. **Courtneidge, S. A., A. D. Levinson, and J. M. Bishop.** 1980. The protein encoded by the transforming gene of avian sarcoma virus ($pp60^{src}$) and a homologous protein in normal cells ($pp60^{proto\text{-}src}$) are associated with the plasma membrane. Proc. Natl. Acad. Sci. U.S.A. **77**:3783–3787.
10. **DeFeo, D., M. A. Gonda, H. A. Young, E. H. Chang, D. R. Lowy, E. M. Scolnick, and R. W. Ellis.** 1981. Analysis of two divergent rat genomic clones homologous to the transforming gene of Harvey murine sarcoma virus. Proc. Natl. Acad. Sci. U.S.A. **78**:3328–3332.
11. **Der, C. J., T. G. Krontiris, and G. M. Cooper.** 1982. Transforming genes of human bladder and lung carcinoma cell lines are homologous to the *ras* genes of Harvey and Kirsten sarcoma viruses. Proc. Natl. Acad. Sci. U.S.A. **79**:3637–3640.
12. **Dhar, R., R. W. Ellis, T. Y. Shih, S. Oroszlan, B. Shapiro, J. Maizel, D. Lowy, and E. Scolnick.** 1982. Nucleotide sequence of the p21 transforming protein of Harvey murine sarcoma virus. Science **217**:934–936.
13. **Eckhart, W., M. A. Hutchinson, and T. Hunter.** 1979. An activity phosphorylating tyrosine in polyoma T antigen immunoprecipitates. Cell **18**:925–933.
14. **Fasano, O., D. Birnbaum, L. Edlund, J. Fogh, and M. Wigler.** 1984. New human transforming genes detected by a tumorigenicity assay. Mol. Cell. Biol. **4**:1695–1705.
15. **Fincham, V. J., D. J. Chiswell, and J. A. Wyke.** 1982. Mapping of nonconditional and conditional mutants in the *src* gene of Prague strain Rous sarcoma virus. Virology **116**:72–83.
16. **Furth, M. E., L. J. Davis, B. Fleurdelys, and E. M. Scolnick.** 1982. Monoclonal antibodies to the p21 products of the transforming gene of Harvey murine sarcoma virus and of a cellular *ras* gene family. J. Virol. **43**:294–304.
17. **Garber, E. A., J. G. Krueger, H. Hanafusa, and A. R. Goldberg.** 1983. Only membrane-associated RSV-src proteins have amino-terminally bound lipid. Nature (London) **302**:161–163.
18. **Gruss, P., R. W. Ellis, T. Y. Shih, M. Konig, E. M. Scolnick, and G. Khoury.** 1981. SV40 recombinant molecules express the gene encoding p21 transforming protein of Harvey murine sarcoma virus. Nature (London) **293**:486–488.
19. **Hager, G. L., E. H. Chang, H. W. Chan, C. F. Garon, M. A. Israel, M. A. Martin, E. M. Scolnick, and D. R. Lowy.** 1979. Molecular cloning of the Harvey sarcoma virus closed circular intermediates: initial structural and biological characterization. J. Virol. **31**:795–809.
20. **Hampar, B., J. G. Derge, A. L. Boyd, M. A. Tainsky, and S. D. Showalter.** 1981. Herpes simplex virus (type 1) thymidine kinase gene does not transform cells morphologically. Proc. Natl. Acad. Sci. U.S.A. **78**:2616–2619.
21. **Henderson, L. E., H.C. Krutzsch, and S. Oroszlan.** 1983. Myristyl amino-terminal acylation of murine retrovirus proteins: an unusual post-translational protein modification. Proc. Natl. Acad. Sci. U.S.A. **80**:339–343.
22. **Jainchill, J. L., S. A. Aaronson, and G. J. Todaro.** 1969. Murine sarcoma and leukemia viruses: assay using clonal lines of contact-inhibited mouse cells. J. Virol. **4**:549–553.
23. **Laemmli, U. K.** 1970. Cleavage of structural proteins during the assembly of the head of bacteriophage T4. Nature (London) **227**:680–685.
24. **Lowry, O. H., N. J. Rosebrough, A. L. Farr, and R. J. Randall.** 1951. Protein measurement with the Folin phenol reagent. J. Biol. Chem. **193**:265–275.
25. **Papageorge, A., D. Lowy, and E. M. Scolnick.** 1982. Comparative biochemical properties of the p21 *ras* molecules coded for by viral and cellular *ras* genes. J. Virol. **44**:509–519.
26. **Parada, L. F., C. J. Tabin, C. Shih, and R. A. Weinberg.** 1982. Human EJ bladder carcinoma oncogene is a homologue of Harvey sarcoma virus *ras* gene. Nature (London) **297**:474–478.
27. **Reddy, E. P., R. K. Reynolds, E. Santos, and M. Barbacid.** 1982. A point mutation is responsible for the acquisition of transforming properties by the T24 human bladder carcinoma oncogene. Nature (London) **300**:148–152.
28. **Rowe, W. P., W. E. Pugh, and J. W. Hartley.** 1970. Plaque assay techniques for murine leukemia viruses. Virology **42**:1136–1139.
29. **Santos, E., S. R. Tronick, S. A. Aaronson, S. Pulciani, and M. Barbacid.** 1982. T24 human bladder carcinoma oncogene is an activated form of the normal human homologue of BALB- and Harvey-MSV transforming genes. Nature (London) **298**: 343–347.
30. **Schlesinger, M. J., A. I. Magee, and M. F. G. Schmidt.** 1980. Fatty acid acylation of proteins in cultured cells. J. Biol. Chem.

255:10021–10024.
31. **Schmidt, M. F. G., and M. J. Schlesinger.** 1979. Fatty acid binding to vesicular stomatitus virus glycoprotein: a new type of post-translational modification of the viral glycoprotein. Cell **17**:813–819.
32. **Schmidt, M. F. G., and M. J. Schlesinger.** 1980. Relation of fatty acid attachment to the translation and maturation of vesicular stomatitus and Sindbis virus membrane glycoproteins. J. Biol. Chem. **255**:3334–3339.
33. **Schultz, A. M., and S. Oroszlan.** 1983. In vivo modification of retroviral *gag* gene-encoded polyproteins by myristic acid. J. Virol. **46**:355–361.
34. **Schultz, A. M., and S. Oroszlan.** 1984. Myristylation of gag-onc fusion proteins in mammalian transforming viruses. Virology **133**:431–437.
35. **Schwab, M., K. Alitalo, H. E. Varmus, J. M. Bishop, and D. George.** 1983. A cellular oncogene (c-Ki-*ras*) is amplified, overexpressed, and located within karyotypic abnormalities in mouse adrenocortical tumour cells. Nature (London) **303**:497–501.
36. **Scolnick, E. M., A. G. Papageorge, and T. Y. Shih.** 1979. Guanine nucleotide-binding activity as an assay for the *src* protein of rat-derived murine sarcoma viruses. Proc. Natl. Acad. Sci. U.S.A. **76**:5355–5359.
37. **Scolnick, E. M., J. R. Stephenson, and S. A. Aaronson.** 1972. Isolation of temperature-sensitive mutants of murine sarcoma virus. J. Virol. **10**:653–657.
38. **Sefton, B. M., I. S. Trowbridge, J. A. Cooper, and E. M. Scolnick.** 1982. The transforming proteins of Rous sarcoma virus, Abelson sarcoma virus, and Harvey sarcoma virus contain tightly-bound lipid. Cell **31**:465–474.
39. **Shih, T. Y., A. G. Papageorge, P. E. Stokes, M. O. Weeks, and E. M. Scolnick.** 1980. Guanine nucleotide-binding and autophosphorylating activities associated with the $p21^{src}$ protein of Harvey murine sarcoma virus. Nature (London) **287**:686–691.
40. **Shih, T. Y., P. E. Stokes, G. W. Smythers, R. Dhar, and S. Oroszlan.** 1982. Characterization of the phosphorylation sites and the surrounding amino acid sequences of the p21 transforming proteins coded for by the Harvey and Kirsten strains of murine sarcoma viruses. J. Biol. Chem. **257**:11767–11773.
41. **Shih, T. Y., M. O. Weeks, P. Gruss, R. Dhar, S. Oroszlan, and E. M. Scolnick.** 1982. Identification of a precursor in the biosynthesis of the p21 transforming protein of Harvey murine sarcoma virus. J. Virol. **42**:253–261.
42. **Shih, T. Y., M. O. Weeks, H. A. Young, and E. M. Scolnick.** 1979. p21 of Kirsten murine sarcoma virus is thermolabile in a viral mutant temperature sensitive for the maintenance of transformation. J. Virol. **31**:546–556.
43. **Shih, T. Y., M. O. Weeks, H. A. Young, and E. M. Scolnick.** 1979. Identification of a sarcoma virus-coded phosphoprotein in nonproducer cells transformed by Harvey or Kirsten murine sarcoma virus. Virology **96**:64–79.
44. **Shimizu, K., M. Goldfarb, M. Perucho, and M. Wigler.** 1983. Isolation and preliminary characterization of the transforming gene of a human neuroblastoma cell line. Proc. Natl. Acad. Sci. U.S.A. **80**:383–387.
45. **Shimizu, K., M. Goldfarb, Y. Suard, M. Perucho, Y. Li, T. Kamata, J. Feramisco, E. Stavnezer, J. Fogh, and M. Wigler.** 1983. Three human transforming genes are related to the viral *ras* oncogenes. Proc. Natl. Acad. Sci. U.S.A. **80**:2112–2116.
46. **Spandidos, D. A., and N. J. Agnantis.** 1984. Human malignant tumours of the breast, as compared to their respective normal tissue have elevated expression of the Harvey *ras* oncogenes. Anticancer Res. **4**:269–272.
47. **Szybalska, E. H., and W. Szybalski.** 1962. Genetics of human cell lines. IV. DNA-mediated heritable transformation of a biochemical trait. Proc. Natl. Acad. Sci. U.S.A. **48**:2026–2034.
48. **Tabin, C. J., S. M. Bradley, C. I. Bargmann, R. A. Weinberg, A. G. Papageorge, E. M. Scolnick, R. Dhar, D. R. Lowy, and E. H. Chang.** 1982. Mechanism of activation of a human oncogene. Nature (London) **300**:143–148.
49. **Taparowsky, E., Y. Suard, O. Fasano, K. Shimizu, M. Goldfarb, and M. Wigler.** 1982. Activation of the T24 bladder carcinoma transforming gene is linked to a single amino acid change. Nature (London) **300**:762–765.
50. **Troxler, D. H., J. K. Boyars, W. P. Parks, and E. M. Scolnick.** 1977. Friend strain of spleen focus-forming virus: a recombinant between mouse type-C ecotropic viral sequences and sequences related to xenotropic virus. J. Virol. **22**:361–372.
51. **Tsuchida, N., and T. Ryder.** 1982. Nucleotide sequence of the oncogene encoding the p21 transforming protein of Kirsten murine sarcoma virus. Science **217**:937–939.
52. **Wei, C.-M., M. Gibson, P. G. Spear, and E. M. Scolnick.** 1981. Construction and isolation of a transmissible retrovirus containing the *src* gene of Harvey murine sarcoma virus and the thymidine kinase gene of Herpes simplex virus type 1. J. Virol. **39**:935–944.
53. **Wierenga, R. K., and W. G. Hol.** 1983. Predicted nucleotide-binding properties of p21 protein and its associated cancer variant. Nature (London) **302**:842–844.
54. **Willingham, M., I. Pastan, T. Y. Shih, and E. M. Scolnick.** 1980. Localization of the *src* gene product of the Harvey strain of murine sarcoma virus to the plasma membrane of transformed cells by electron microscopic immunocytochemistry. Cell **19**:1005–1014.
55. **Willumsen, B., A. Christensen, N. L. Hubbert, A. G. Papageorge, and D. Lowy.** 1984. The p21 *ras* C-terminus is required for transformation and membrane association. Nature (London) **310**:583–586.